



1 Spatial and temporal variability of methane emissions and 2 environmental conditions in a hyper-eutrophic fishpond

3 Petr Znachor^{1,2}, Jiří Nedoma¹, Vojtech Kolar^{1,3}, Anna Matoušů¹

4 ¹Biology Centre of Czech Academy of Sciences, v.v.i., Institute of Hydrobiology, Na Sádkách 7, České
5 Budějovice, 37005, Czech Republic

6 ²Faculty of Science, University of South Bohemia, Branišovská 1760, České Budějovice, 37005, Czech Republic

7 ³Biology Centre of Czech Academy of Sciences, Institute of Entomology, Branišovská 31, České Budějovice, 370
8 05, Czech Republic

9

10 *Correspondence to:* Anna Matoušů (anna.matousu@gmail.com)

11

12 **Abstract.** Estimations of methane (CH₄) emissions are often based on point measurements using either flux
13 chambers or a transfer coefficient method which may lead to strong underestimation of the total CH₄ fluxes. In
14 order to demonstrate more precise measurements of the CH₄ fluxes from an aquaculture pond, using higher
15 resolution sampling approach we examined the spatiotemporal variability of CH₄ concentration in the water,
16 related fluxes (diffusive and ebullitive) and relevant environmental conditions (temperature, oxygen, chlorophyll-
17 a) during three diurnal campaigns in a hyper-eutrophic fishpond. Our data show remarkable variance spanning
18 several orders of magnitude while diffusive fluxes accounted for only a minor fraction of total CH₄ fluxes (4.1–
19 18.5 %). Linear mixed-effects models identified water depth as the only significant predictor of CH₄ fluxes. Our
20 findings necessitate complex sampling strategies involving temporal and spatial variability for reliable estimates
21 of the role of fishponds in a global methane budget.

22

23 **Keywords:** aquaculture, emissions, fishpond, freshwater, heterogeneity, methane

24



25 **1 Introduction**

26 Freshwater aquaculture ponds (fishponds) represent man-made counterparts to natural shallow lakes (Scheffer,
27 2004) which are mainly used for fish production (mostly of common carp, *Cyprinus carpio* L.) and water retention
28 in the landscape. Fishponds serve also as secondary biotope for various organisms (Kolar et al., 2021), supporting
29 noteworthy animal and plant diversity (Pokorný and Hauser, 2002). However, most fishponds suffer from high
30 fish stock densities, excessive carbon and nutrient loading from supplemental fish feeding, sewage pollution, and
31 fertiliser runoffs from agricultural catchments or nutrient mobilisation from the anoxic sediment layers (Pechar,
32 2000). As a result, the trophic structure of plankton communities has shifted towards a reduction of large
33 zooplankton and massive development of phytoplankton, especially cyanobacterial blooms (Potužák et al., 2007),
34 limiting light penetration in the water column. Rapid changes in the intensity of biological processes such as
35 photosynthesis and respiration often result in pronounced daily or seasonal fluctuations in dissolved oxygen (Baxa
36 et al., 2021), signalling decreasing ecosystem stability. The extent of anoxia, accumulation of organic biomass,
37 and rapid heating of the shallow water during summer result in enhanced production of greenhouse gases (Grasset
38 et al., 2018, Zhang et al., 2021; Bartosiewicz et al., 2021).

39 Most concerning are CH₄ emissions as freshwater aquaculture systems release more than 6 Tg CH₄ yr⁻¹ (Yuan et
40 al., 2019). Methane can be emitted via several pathways: simple molecular diffusion, ebullition (in the form of
41 bubbles released from oversaturated sediments), plant-mediated flux (Bastviken et al., 2004), but also through so
42 far neglected pathways including aeration, emissions from dry/drying sediments, or dredged organic material
43 (Kosten et al., 2020). Among all, ebullition is considered the dominant pathway (van Bergen et al., 2019; Kosten
44 et al., 2020), which can contribute 50-96 % (Casper et al., 2000; Xiao et al., 2017; van Bergen et al., 2019; Yang
45 et al., 2020; Zhao et al., 2021) to the total CH₄ flux. Along with the second important pathway – molecular
46 diffusion, both exhibit high spatiotemporal variability due to various physical and biological factors acting on very
47 short time scales, for instance, temperature (van Bergen et al., 2019), eutrophication (Zhang et al., 2021), water
48 depth (DelSontro et al., 2016), CH₄ production rates (Zhou et al., 2019), CH₄ oxidation rates (Sanseverino et al.,
49 2013), dissolved oxygen concentration (Xiao et al., 2017), management regime (Yang et al., 2019), or the quality
50 of organic matter in the sediment (Schmiedeskamp et al., 2021). Recently, the direct involvement of phytoplankton
51 in CH₄ production and emissions has been emphasised (Yan et al., 2019; Bižić et al., 2020; Bartosiewicz et al.,
52 2021).



53 Although fishponds are recognised as powerful model systems for studies in ecology and evolutionary or
54 conservation biology (De Meester et al., 2005; Céréghino et al., 2008), the extent of environmental heterogeneity
55 in fishponds and shallow Inland small waterbodies remains poorly understood (Ortiz and Wilkinson, 2021), largely
56 because the driving factors are either system-specific or highly variable on short time scales (Laas et al., 2012).
57 Most of current information on lentic ecosystem structure and function comes from single-site sampling, in which
58 measurements are taken over time at the deepest point in the lake, which does not sufficiently account for within-
59 lake spatial variation (Stanley et al., 2019). The motivation for our study was the growing concern about the role
60 of fishponds as important sources of CH₄ fluxes to the atmosphere (Wik et al., 2016). Unfortunately, the majority
61 of global CH₄ flux estimates rely on upscaling methods (DelSontro et al., 2018a) based on a limited number of
62 measurements that do not account for diurnal and seasonal variability or ecosystem spatial heterogeneity. Yang et
63 al. (2019) indicates that a larger number of spatial replicates over a number of months is mandatory to improve
64 the accuracy of whole-pond CH₄ flux estimates. The published research from other aquaculture studies have been
65 performed mainly in tropical and subtropical zones in fish or crab aquacultures (e.g., Hu et al., 2016; Ma et al.,
66 2018; Yang et al., 2019, 2020; Yuan et al., 2019, 2021). To better understand the spatial dynamics of CH₄ fluxes
67 and environmental heterogeneity in temperate freshwater shallow lake, we conducted a spatial sampling of the
68 hyper-eutrophic Dehtář fishpond (Czech Republic, Europe). Since the seasonal CH₄ production is strongly affected
69 by temperature, we focused on warm summer months where the total CH₄ fluxes were expected to be the highest
70 (Jansen et al., 2020). The objectives of our study were (i) to determine the spatial heterogeneity of CH₄ diffusive
71 and total fluxes and fundamental limnological variables (oxygen, temperature, chlorophyll-a) and they change
72 daily and monthly in the hyper-eutrophic pond, and (ii) to identify the factors that influence CH₄ fluxes to improve
73 our understanding of the importance of spatiotemporal variability for global estimates of CH₄ efflux to the
74 atmosphere.

75 **2 Material and Methods**

76 **2.1 Study site description**

77 The Dehtář fishpond (49° N, 14° E) is a shallow man-made lake (average and maximum depth: 2.4 and 6 m)
78 constructed in 1479 and used for polycultural, semi-intensive production of common carp (Potužák et al., 2016).
79 It lies in a flat agricultural landscape at 406.4 m above sea level in the upper Vltava River basin in South Bohemia
80 (Czech Republic) which is characteristic with its network of fishponds (Fig. 1b). Due to the orography of the



81 landscape, the Dehtář fishpond, surrounded by narrow belts of littoral vegetation and adjacent to grassland and
82 arable land, is exposed to wind, mainly from the northwest (for aerial photograph, see Suppl. Fig 1). The catchment
83 area is 91.4 km². The main inflow is the Dehtářský stream in the south, while several smaller tributaries flow in
84 from the west (Fig. 1c). The fishpond has a dam 234 m long and 10 m high, with two outlets and a safety spillway.
85 Covering 2.28 km², the Dehtář fishpond is among the ten largest fishponds in the Czech Republic, holding a
86 volume of 4.71×10^3 m³ and having a water residence time of 146-445 days (Potužák et al., 2016).



87

88 **Figure 1.** Location (a, b; copyright www.d-maps.com; https://d-maps.com/carte.php?num_car=2232&lang=en and https://d-maps.com/carte.php?num_car=265046&lang=en; modified) and bathymetric map (c; credit Jiří Jarošík) of the sampled Dehtář
89 fishpond; Blue lines indicate hydrological connections; red dots are the sampling points. Numbers indicate isobath depth.
90

91

92 2.2 Sampling design and measurement

93 To measure spatial heterogeneity and temporal changes in limnological parameters and methane fluxes, we
94 conducted three 36-hour surveys in summer 2019 (July 2-3, August 13-14, September 19-20). In the morning
95 (between 5-6 a.m.), we first measured surface values and vertical profiles of temperature, oxygen, and chlorophyll-
96 *a* concentration at the deepest point (see below for details). We subsequently installed 15 floating polyethylene
97 gas chambers (as shown in Fig. 1c), serving as fixed sampling sites and at the same time for accumulation of CH₄
98 fluxes (see further), starting in the western part of the fishpond. During installation (and further during each



99 sampling), temperature, pH, and oxygen concentration were measured at 0.3 m depth using the WTW 330i pH
100 meter and Oximeter (WTW, Weilheim, Germany). Vertical chlorophyll-*a* profiles were measured at each sampling
101 site using a submersible fluorescence probe (FluoroProbe, bbe-Moldaenke, Kiehl, Germany). From each site, the
102 average chlorophyll-*a* concentration in the surface layer (0-1 m depth) was used to assess the phytoplankton spatial
103 heterogeneity.

104 To minimise the chance that the differences observed among sites were due to time of day, we conducted repeated
105 measurements at the deepest point at the end of each sampling. If there was a change, all values were corrected for
106 the sampling time by linear interpolation:

$$107 \quad P_{corr} = P_t + (P_{end} - P_0) \times \frac{(t-t_0)}{(t_{end}-t_0)} \quad (1)$$

108 where P_{corr} is the corrected value of a parameter, P_t is its value measured at the time t , P_0 and P_{end} are parameter
109 values measured at the deepest point at the start (time t_0) and at the end (t_{end}) of the sampling. In the evening and
110 morning of the second day (roughly at 12 h intervals), we performed additional measurements of spatial
111 heterogeneity, allowing us to assess diurnal and nocturnal changes. In addition, samples for measuring CH_4
112 concentration in the surface water were collected at each site and analysed as described below. To assess diurnal
113 variations in thermal structure and oxygen concentration in the water column, we made vertical profile
114 measurements at the deepest point at 3-6 h intervals using the YSI EXO 2 multiparametric probe (YSI Inc., Yellow
115 Springs, USA).

116 **2.3 Methane measurements**

117 Water samples for determining CH_4 concentration in the surface water were collected at all 15 sampling sites in
118 triplicates into 20 ml glass bottles. The bottles were capped bubble-free under water with black butyl rubber
119 stoppers (Ochs, Germany) and sealed with aluminium crimps. Immediately after sampling, the water samples were
120 preserved by injecting 100 μ l of concentrated sulfuric acid to stop the microbial activity (Bussmann et al., 2015).
121 The samples were processed within one week in the laboratory using a headspace technique according to
122 McAuliffe (1971). Methane concentration in the headspace was measured using an HP 5890 Series II gas
123 chromatograph (Agilent Technologies, USA) and calculated with the solubility coefficient given by Yamamoto et
124 al. (1976).

125 Methane diffusive fluxes (F) were then calculated for each sampling site indirectly using the 2-layer model with
126 the equation:

$$127 \quad F = k(C_{sur} - C_{eq}) \quad (2)$$



128 where C_{sur} is the CH_4 concentration in surface water in $\mu\text{mol L}^{-1}$, C_{eq} is the CH_4 concentration in surface water in
129 equilibrium with the atmosphere in $\mu\text{mol L}^{-1}$, and k is the CH_4 exchange constant (cm h^{-1}). The value of k was
130 calculated from the local wind speed according to Crusius and Wanninkhof (2003):

$$131 \quad k = k_{600} \left(\frac{Sc}{600} \right)^n \quad (3)$$

132 where k_{600} is the gas transfer velocity for a Schmidt number (Sc) of 600. The Schmidt number for CH_4 was
133 calculated according to Wanninkhof (2014):

$$134 \quad Sc = 1909.4 - 120.78t + 4.1555t^2 - 0.080578t^3 + 0.000658t^4 \quad (4)$$

135 where t ($^{\circ}\text{C}$) is the water temperature at the time of CH_4 extraction. The parameter C_{eq} in Eq. (1) was determined
136 from the equation:

$$137 \quad C_{\text{eq}} = \beta \times p\text{CH}_4 \quad (5)$$

138 where β is the solubility coefficient of CH_4 as a function of temperature according to Wiesenburg and Guinasso
139 (1979), and $p\text{CH}_4$ is the partial pressure of CH_4 in the atmosphere.

140 To estimate total CH_4 fluxes from the water column to the atmosphere (i.e., diffusive and ebullitive fluxes), we
141 measured CH_4 accumulation in open-bottom floating polyethylene chambers (volume 3.1 L; area 0.024 m^2). Each
142 gas chamber was anchored at individual 15 fixed sampling sites, but allowed to float freely on the water surface.
143 Gas was accumulating for approximately 12 h during each sampling period, i.e., during the day and night periods.
144 Afterwards, 30 ml of gas was carefully taken from each chamber, after mixing the headspace in the chamber, and
145 stored in evacuated Exetainers[®] (Labco Limited, UK). Chambers were ventilated after each sampling period to
146 reset the incubation conditions. Methane fluxes were calculated as the difference between initial background and
147 final concentration in the chamber headspace and expressed on the 1 m^2 area of the surface level per day according
148 to Bastviken et al. (2004).

149 **2.4 Background limnological parameters**

150 During each campaign, samples for analysis of nutrient concentration and phytoplankton composition were
151 collected from the surface at the deepest point using a Friedinger sampler. Water transparency was measured using
152 a Secchi disk. Total phosphorus (TP) and soluble reactive phosphorus (SRP) were analysed
153 spectrophotometrically according to Kopáček and Hejzlar (1993) and Murphy and Riley (1962), respectively.
154 Concentrations of NH_4^+ and NO_3^- were determined according to the procedure of Kopáček and Procházková
155 (1993) and Procházková (1959), respectively. Phytoplankton samples were preserved with Lugol's solution and



156 examined for species composition with an inverted microscope (Olympus IMT-2). Weather data were obtained
157 from the gauging station at the fishpond dam.

158 **2.5 Statistical analyses**

159 Two-tailed paired Student's t-tests and Two-way ANOVA with post-hoc Tukey's multiple comparison test (Prism
160 9.3, GraphPad Software Inc., La Jolla, USA) tested for differences between diffusive and total CH₄ fluxes between
161 day and night and among three sampling campaigns, respectively. The percentage of data variability explained by
162 different factors (daytime, month and site) was calculated with the Two-way RM ANOVA. Contour graphs
163 illustrating changes in spatial heterogeneity of measured parameters were constructed in Surfer 10 (Golden
164 Software, Inc., Colorado, USA) using the kriging contouring method. Spatial heterogeneity was quantified by
165 calculating the spatial variance (i.e., coefficient of variation):

$$166 \quad CV\% = 100 \times \frac{SD}{mean} \quad (6)$$

167 Higher spatial variance indicates increasing ecosystem patchiness. Linear mixed-effects models were used to
168 analyse the effects of O₂, pH, temperature, and water depth on the CH₄ diffusive fluxes with the random effect of
169 time of day nested within the effect of sampling date. The most parsimonious model was obtained by a manual
170 backward selection, where we sequentially removed all insignificant predictors ($p > 0.05$) using likelihood ratio
171 tests implemented in the drop1 function (Zuur et al., 2009). We also compared the slopes of the month-specific
172 regression lines produced by the model using analysis of covariance (Zar, 1984). Linear mixed-effects models
173 were implemented in the lme4 package version 1.1-21 (Bates et al., 2015), and Kenward-Roger F-tests were
174 computed using the ANOVA Type II function from the pbkrtest package version 0.4-7 (Halekoh and Hojsgaard,
175 2014). The prediction of the resulting final model was visualised in the package ggeffects version 0.14.1 (Lüdecke,
176 2018). Package performance version 0.4.4 (Lüdecke et al., 2020) was used to calculate Nakagawa's R² of the linear
177 model. The statistical analyses were performed using R software (v. 3.5.2, R Core Team, 2018).

178 **3 Results**

179 **3.1 Weather and background fishpond characteristics**

180 Weather parameters varied among sampling campaigns. In July, clear skies prevailed with the daily air temperature
181 above 30 °C (Table 1). During the August and September measurements, it was very cloudy, and daily air
182 temperatures decreased to 22 and 18 °C, respectively. The water level was stable during the whole studied period



183 with a monthly fluctuation of ~ 10 cm. Water transparency was low (15-40 cm), with an increasing trend towards
184 the end of summer (Table 1). Concentrations of total phosphorus and soluble reactive phosphorus were high (Table
185 1), consistent with a hyper-eutrophic state of the fishpond. In contrast, nitrogen concentrations were rather low,
186 with ammonium nitrogen being the predominant form of inorganic N in the water (Table 1).

187 **Table 1:** Basic characteristics of the Dehtář fishpond during the studied period.

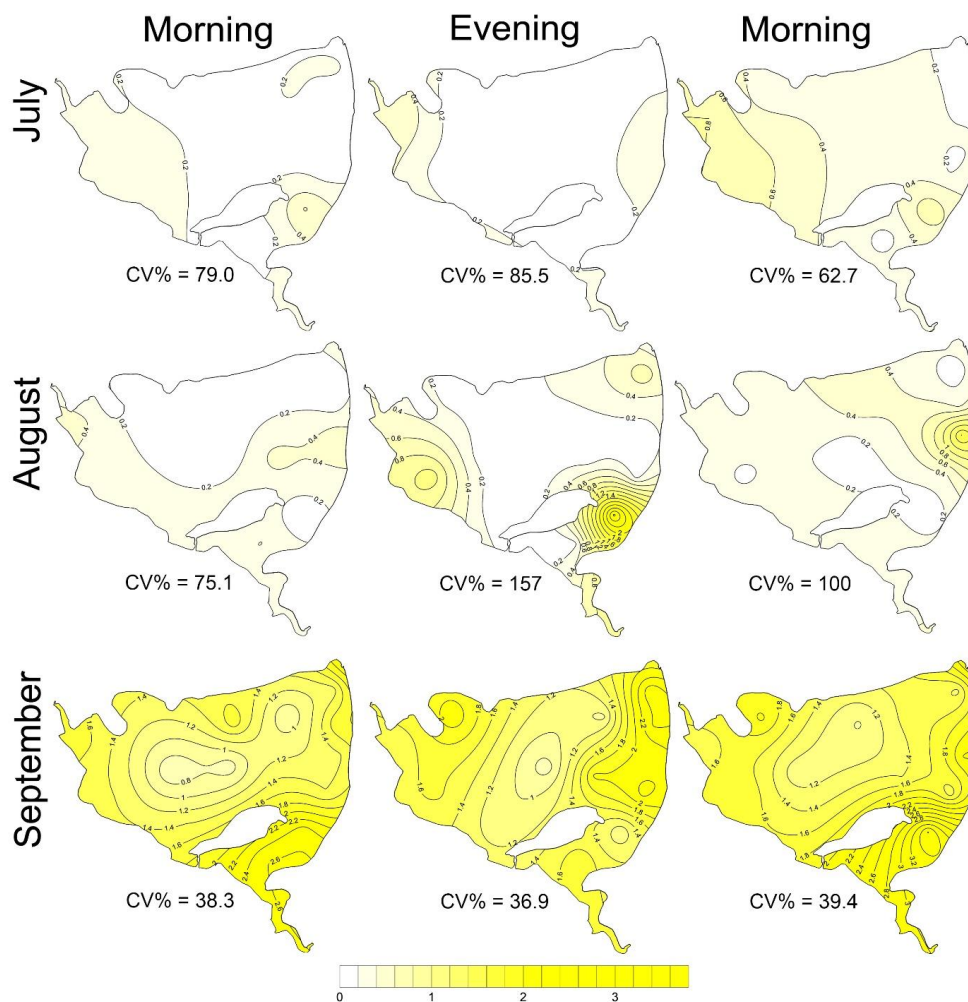
	July	August	September
Weather	Clear sky, windy	Partly cloudy, no wind	Partly cloudy, no wind
Air temperature (°C)	25-32	20-22	11-18
PHAR (mol m⁻² day⁻¹)	9.5	3.4	5.0
Secchi depth (cm)	15	30	40
TP (µg l⁻¹)	568	527	406
SRP (µg l⁻¹)	100	200	107
N-NH₄⁺ (µg l⁻¹)	23	783	560
N-NO₃⁻ (µg l⁻¹)	14	23	46
Chl-<i>a</i> (µg l⁻¹)	456	156	185
Phytoplankton composition	Cyanobacteria	Cyanobacteria, green algae, cryptophytes	Cryptophytes, green algae

188
189 Chlorophyll-*a* concentrations were highest in July due to the dense cyanobacterial bloom accumulated at the
190 surface (Table 1). The phytoplankton consisted of only three cyanobacterial taxa: *Dolichospermum flos-aquae*,
191 *Planktothrix agardhii*, and *Raphidiopsis mediteranea*. In August, phytoplankton was more diverse but also
192 dominated by cyanobacteria: *P. agardhii*, *Aphanizomenon issatschenkoi*, and *D. flos-aquae*. In September,
193 cyanobacteria were absent and instead, cryptophytes (*Cryptomonas reflexa*), green algae (*Pediastrum*, *Coelastrum*
194 and *Desmodesmus*) and dinoflagellates (*Ceratium hirundinella*) prevailed.

195 3.2 Methane concentration and fluxes

196 The CH₄ concentration in surface water was highly supersaturated over the whole studied period. The obtained
197 values varied from 0.003 up to 3.75 µmol L⁻¹ (Fig. 2), which corresponded to saturation levels of 108-12 834%. It
198 is obvious, that the obtained data show remarkable variance: the mean (± SD) values were 0.22 ± 0.18 for July,
199 0.34 ± 0.45 for August, and 1.61 ± 0.61 µmol L⁻¹ for September (Suppl. Fig. 11).

200

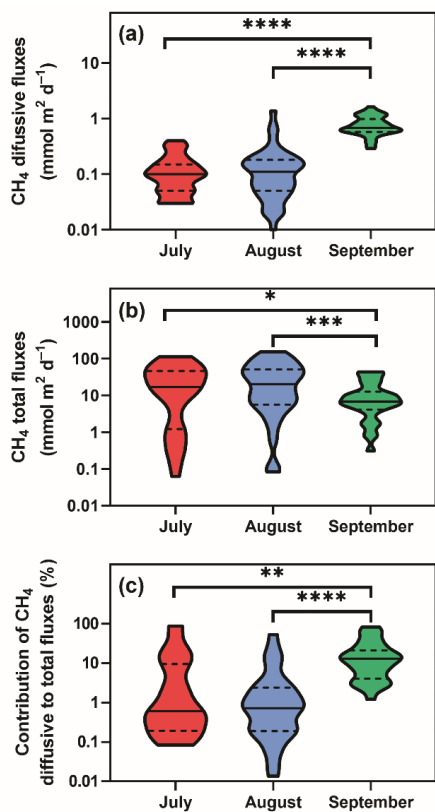


201

202 **Figure 2:** Contour graphs illustrating both seasonal and daily changes in spatial heterogeneity (indicated by the coefficient of
203 variation, CV%) of the surface methane concentration ($\mu\text{mol L}^{-1}$) in the fishpond.

204

205 Diffusive fluxes (i.e., calculated from CH_4 concentration, see Eq. 2) showed the lowest values in July and August
206 (average 0.12 and $0.16 \text{ mmol m}^{-2} \text{ d}^{-1}$, respectively) and pronouncedly peaked in September (average 0.78 mmol
207 $\text{m}^{-2} \text{ d}^{-1}$, Fig. 3a). By contrast, in July and August, the average total CH_4 fluxes (obtained with floating chambers)
208 showed the highest values (average $31.8 \text{ mmol m}^{-2} \text{ d}^{-1}$; ranging from 0.08 to $152 \text{ mmol m}^{-2} \text{ d}^{-1}$) while in
209 September, total CH_4 fluxes were three times lower than before (average $11.8 \text{ mmol m}^{-2} \text{ d}^{-1}$, range 0.3 to 43.5
210 $\text{mmol m}^{-2} \text{ d}^{-1}$, Fig. 3b). As a result, diffusive fluxes accounted for only a minor fraction of total CH_4 fluxes to the
211 atmosphere (on average, 9.2% in July, 4.1% in August, 18.5% in September, Fig. 3c).



212

213 **Figure 3:** Violin plots of CH₄ diffusive (a) and total fluxes (b) during the studied period. Panel (c) depicts differences in the
214 percentage contribution of diffusive to total fluxes. Solid lines are medians, while dashed lines denote quartiles. Asterisks
215 indicate significant differences (* p<0.05, ** p<0.01, *** p<0.001, **** p<0.0001) between sampling dates determined by
216 two-way ANOVA with Tukey's multiple comparison test. Note that a log scale is used here for clarity.

217

218 The total CH₄ fluxes show spatial variability within the fishpond that range several orders of magnitude (Fig. 3, 4;
219 Suppl. Fig. 11; Suppl. Table 1). The observed spatial pattern showed high temporal variability on both daily and
220 monthly scales (Fig. 2, 4, Suppl. Table 1). Most of the variability in CH₄ diffusive fluxes was explained by
221 sampling date (62.4 %), while for the total CH₄ fluxes, spatial heterogeneity accounted for 87.2 % of data
222 variability (Table 2). Using linear mixed-effects models, we identified water depth as the only significant predictor
223 of total CH₄ fluxes (Df = 1, p < 0.0001, marginal Nakagawa's R² = 0.348; Fig. 5).

224

225

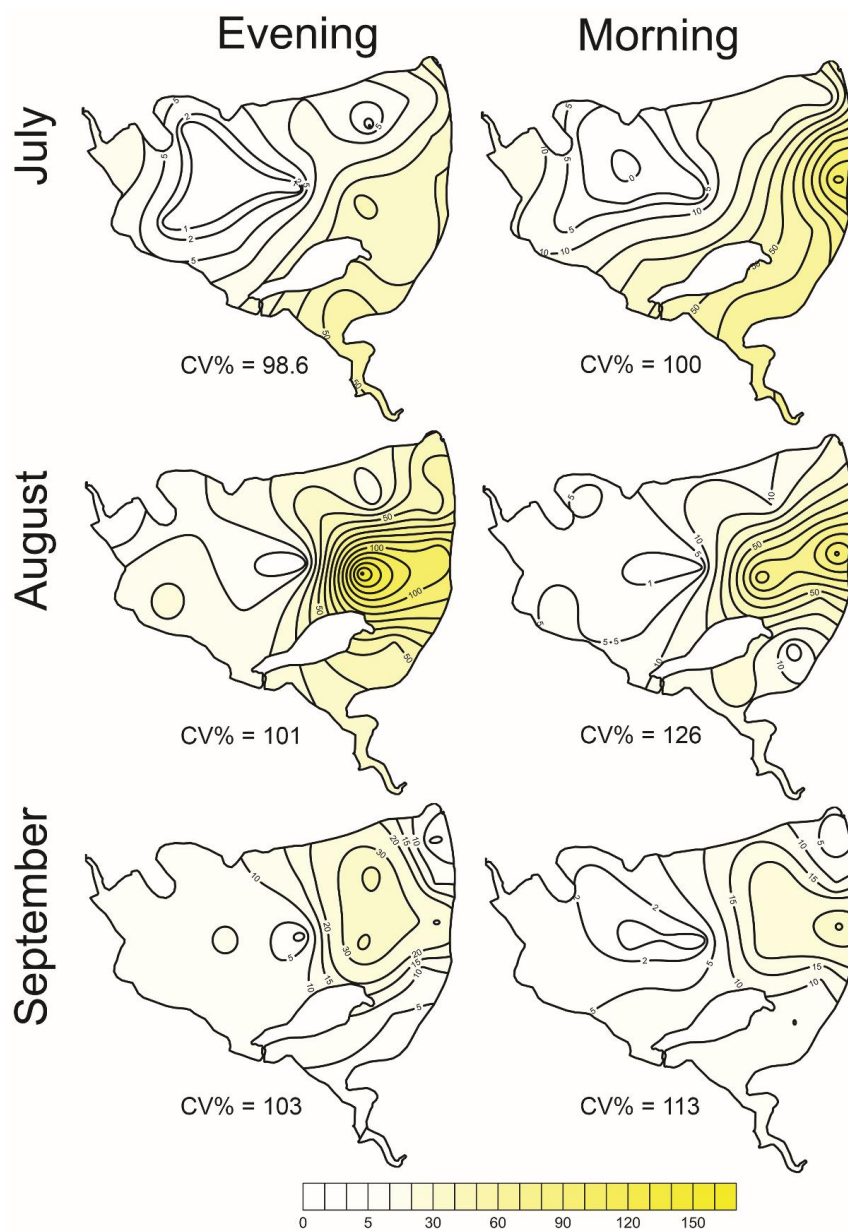
226



227 **Table 2:** The percentage of data variability explained by different factors (daytime, month = sampling date, and site)
 228 calculated with the Two-way RM ANOVA. Statistical significant values ($p < 0.01$) are bold.

	% of variability				Significance		
	Daytime	Month	Site	Unexplained	Daytime	Month	Site
CH₄ diffusive flux	2.3	62.4	13.2	22.1	0.0123	<0.0001	<i>n.s.</i>
CH₄ total flux	0.19	2.4	87.2	10.2	<i>n.s.</i>	<i>n.s.</i>	<0.0001
pH	4.4	64.9	11.1	19.6	0.0001	<0.0001	<i>n.s.</i>
Water temperature	3.3	92.3	2.5	1.9	<0.0001	<0.0001	<0.0001
O₂	21.7	48.1	13.8	16.4	<0.0001	<0.0001	0.0135
Chl-<i>a</i>	0.019	74.9	16.7	8.4	<i>n.s.</i>	<0.0001	<0.0001

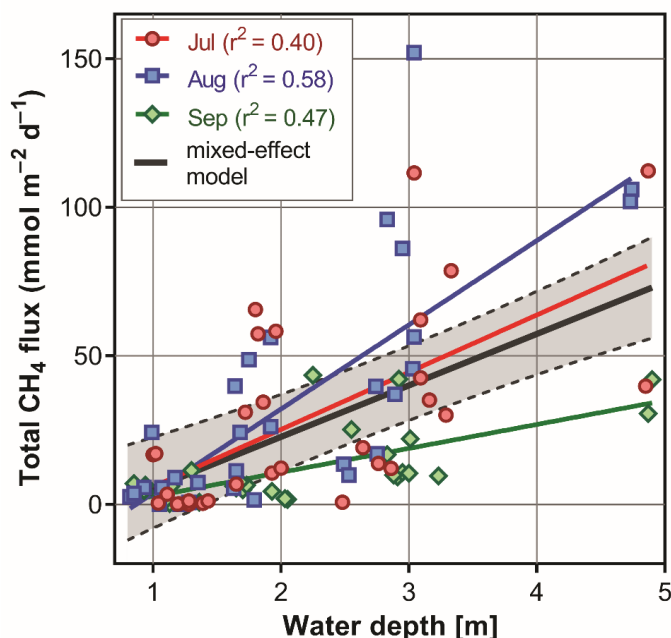
229 Interestingly, slopes of the linear regressions differed significantly among individual sampling campaigns (Fig. 5),
 230 indicating an additional season-related factor that affects CH₄ fluxes in the fishpond. Calculated CH₄ diffusive
 231 fluxes were not correlated with total fluxes. Linear mixed-effects models did not identify any significant predictor
 232 of the fluxes, indicating that factors and processes out of the study's scope are involved. We found no significant
 233 difference in either diffusive or total CH₄ fluxes between day and night.



234

235 **Figure 4:** Contour graphs of methane total fluxes in the Dehtár fishpond. Isopleths connect sites with the same value of
236 methane fluxes ($\text{mmol m}^{-2} \text{day}^{-1}$). CV% is a measure of spatial heterogeneity.

237

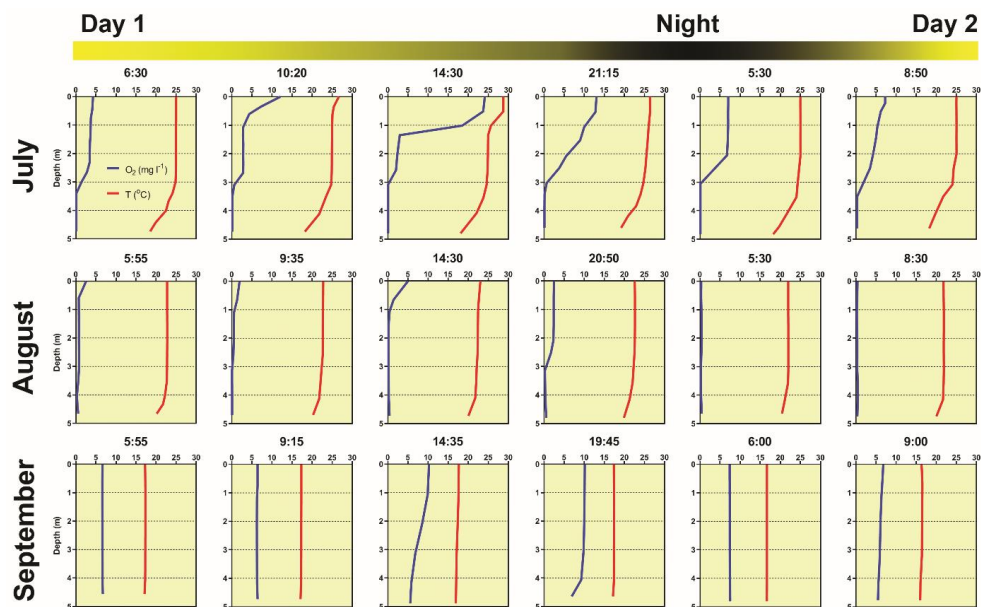


238

239 **Figure 5:** The most parsimonious linear mixed-effect model of methane total fluxes showing the water depth as the only
240 significant predictor. Symbols are the measured values, the solid black line is the prediction, and dashed lines are 95th
241 confidence intervals. Colours indicate month specific relation between total methane fluxes and water depth. Differences in
242 slopes were tested using the F-test. In September, the slope of the regression line was significantly different from that in July
243 and August.

244 3.3 Diurnal changes in vertical profiles of oxygen and temperature

245 Several contrasting patterns of vertical temperature and oxygen profiles occurred during summer 2019. Diurnal
246 changes were most pronounced in July (Fig. 6). Surface temperatures varied from 25 °C in the morning to nearly
247 30 °C in the afternoon. Thermal stratification of the water column was weak in the morning but became strongest
248 at 14:30 with a thermocline at 0.5 m depth (Fig. 6). Later in the afternoon, the water column began to be mixed by
249 wind. The morning vertical oxygen profile was characterised by a surface value of 4.3 mg L⁻¹, corresponding to
250 51 % saturation and anoxia below 3 m.



251

252 **Figure 6:** Diurnal changes in vertical profiles of temperature and oxygen concentration measured at the deepest point of the
253 fishpond. Numbers above each graph indicate the time of measurement.

254 Due to the high photosynthetic activity of cyanobacteria, the surface oxygen concentration increased to 24 mg L^{-1}
255 (320% saturation, Fig. 6), and a steep oxycline was established at a depth of 0.5-1.5 m with no effect on the
256 anoxic conditions at the deeper layers. Wind action eroded both the oxy- and thermoclines in the evening, and by
257 the next morning, the vertical profiles were similar to those at the beginning.

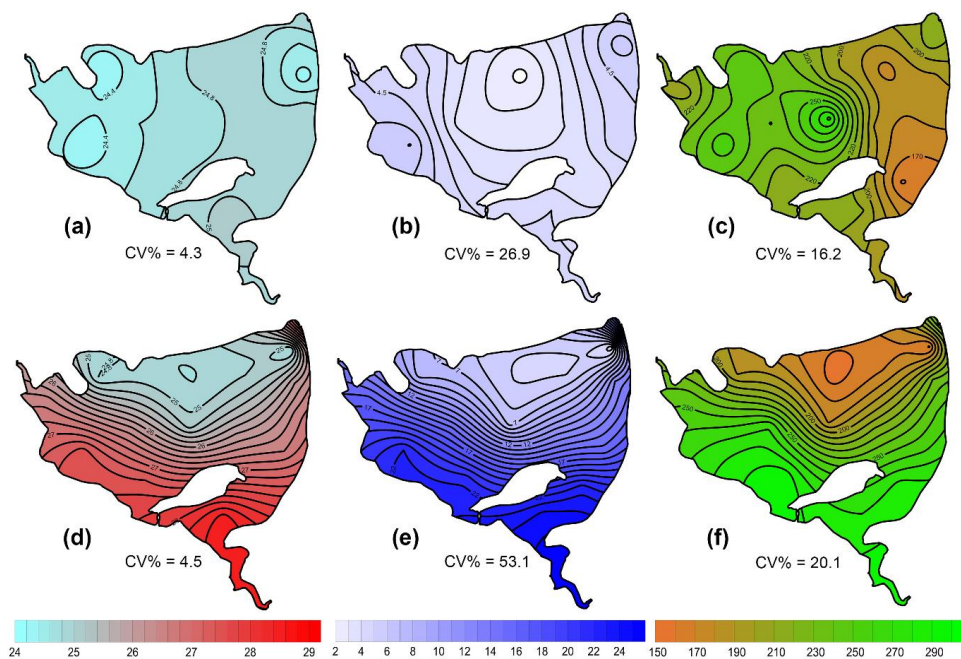
258 In August, the water column was almost entirely mixed and low in oxygen in the morning, with only 2.6 mg L^{-1}
259 (30% saturation) of oxygen at the surface. Due to cloudy weather, the daily photosynthetic activity of
260 phytoplankton resulted in only a slight increase in oxygen concentration at 0-1.5 m depth (4 mg L^{-1} , 47%
261 saturation). By the morning of the next day, the entire water column turned very close to anoxic (0.4 mg L^{-1} , 4%
262 saturation; Fig. 6), which in turn affected the spatial distribution of zooplankton, as evidenced by the formation of
263 dense zooplankton clouds accumulated in the thin layer just at the surface (see Suppl. Fig. 3). In September, the
264 water column was completely mixed, and we observed only weak daily changes in thermal and oxygen vertical
265 structures (Fig. 6).

266 **3.4 Effect of wind on spatial heterogeneity of temperature, oxygen and chlorophyll-*a***

267 During the summer, all measured parameters showed remarkable within-lake spatial heterogeneity (Suppl. Fig. 4-
268 8). In July, meteorological conditions allowed for demonstrating the effect of wind on fishpond spatial



269 heterogeneity. In the morning, there were no substantial differences in the surface temperature and oxygen
270 concentrations (Fig. 7ab). Phytoplankton biomass was accumulated mostly in the shallow western part, with the
271 maximum in the centre (Fig. 6c). At 14:00, a light breeze started to blow from the northwest, achieving a maximum
272 of 11 km h^{-1} (Suppl. Fig. 7). This episode lasted till the evening measurement, and the wind ceased by 21:00. The
273 wind was strong enough to change spatial distribution substantially (Fig. 7d-f, Suppl. Fig. 4). In the evening, the
274 surface water temperature on the windward (south) side of the fishpond was $\sim 4 \text{ }^{\circ}\text{C}$ higher than in the north (Fig.
275 7d). The wind also induced order of magnitude differences in oxygen concentration along the north-south axis of
276 the fishpond (3 mg L^{-1} of O_2 at the north, 24 mg L^{-1} of O_2 at the south; Fig. 7e) and affected phytoplankton
277 distribution in the fishpond, resulting in remarkable bloom accumulation in the south (Fig. 7f, Suppl. Fig. 8).
278 During the calm night after the disturbance, the north-south gradient substantially weakened. In August and
279 September, the thermal heterogeneity of the pond was rather low, but the spatial distribution of oxygen and
280 chlorophyll-*a* remained highly variable (Suppl. Fig. 5–8, Suppl. Table 1).



281

282 **Figure 7:** Contour graphs of surface temperature (a, d; $^{\circ}\text{C}$), oxygen concentration (b, e; mg L^{-1}) and chlorophyll-*a*
283 concentration (c, f; $\mu\text{g L}^{-1}$) measured on July 2 at different times of day: a, b and c are the morning measurements; d, e and f
284 are evening measurements following a wind disturbance. Coefficient of variation (CV %) is a measure of spatial heterogeneity
285 of measured parameters.



286 **Discussion**

287 **4.1 Methane fluxes**

288 Assessing spatial heterogeneity of the CH₄ fluxes within a fishpond is critical for a reliable estimate of its
289 contribution to the global CH₄ budget. In our study, the variability in total CH₄ fluxes spanned several orders of
290 magnitude (ranging from 0.06 up to 1 121.3 mmol m⁻² d⁻¹), which is in agreement with similar studies (Casper et
291 al., 2000; DelSontro et al., 2016; Natchimutu et al., 2016). However, most system-specific CH₄ flux estimates rely
292 on upscaling from a limited number of sites (Bastviken et al., 2004; Rasilo et al., 2015; Wik et al., 2016) because
293 obtaining spatial variability in CH₄ emission is methodologically challenging. In general, spatial heterogeneity
294 may reflect differences in water sources, physical mixing, local transformations and biogeochemical processes and
295 rates among lake habitats (Loken et al., 2019). In deep lakes, littoral areas can contribute disproportionately to
296 total lake CH₄ fluxes (Hofmann et al., 2010; Hofmann 2013, Natchimuthu et al., 2016; Schilder et al., 2013) and
297 are often missed by traditional sampling approaches (Wik et al., 2016). According to Wik et al. (2016), low
298 temporal and spatial resolutions are unlikely to cause overestimates. On the other hand, DelSontro et al. (2018b)
299 suggested that horizontal transport of CH₄ produced in littoral zones and the interaction between physical and
300 biological processes (e.g. air-water gas exchange, water column mixing, the interplay between CH₄ production
301 and microbial oxidation) may result in an underestimation of whole-lake CH₄ fluxes based on centre samples.
302 Similarly, Natchimuthu et al. (2016) found that up to 78 % underestimation would occur if samples obtained only
303 from the lake center are used to extrapolate the total CH₄ flux. However, extrapolating our data from the deepest
304 point of the Dehtář fishpond would lead to an overestimation of the CH₄ fluxes by a factor of 2.9 (Suppl. Fig. 12).
305 The bias introduced by the deepest point measurement appears to be highly variable among systems with different
306 morphology, geographical location, mixing regimes or trophic states. For instance, analysis of 22 European lakes
307 during late summer has shown that spatially resolved CH₄ diffusive fluxes were highly variable for individual
308 lakes, yielding 55–300 % differences in the whole-lake estimates (Schilder et al., 2013). Schmiedeskamp et al.
309 (2021) observed an increase in CH₄ fluxes from the shore towards the centre in response to increasing sediment
310 C-content in two shallow German lakes. In line with these findings, our results provide further evidence that
311 spatially resolved data are needed to validate the uncertainties that come from using single-point samples to
312 represent whole-lake processes in hyper-eutrophic systems. As stated by Loken et al. (2019), rather than assuming
313 spatial homogeneity, scaling-up exercises of global carbon budgets should acknowledge the uncertainty that comes
314 from extrapolating from spatially limited data sets.



315 In the Dehtář fishpond, the total CH₄ fluxes increased with water depth, and this relationship was month specific.
316 The highest CH₄ fluxes at the deepest points may seem contradictory to previous studies, in which the highest
317 fluxes were typically observed in littoral areas (e.g. DelSontro et al., 2018b; Hofman et al., 2010; Natchimuthu et
318 al., 2016; Schilder et al., 2013). However, these findings are based on studying mostly lakes whose morphology,
319 trophic state or oxygen regime sharply contrast with the Dehtář fishpond, where the upper two meters of the water
320 column were oxygen-saturated while the deepest strata were mostly anoxic. In such hyper-eutrophic systems, high
321 nutrient loading increases autochthonous primary production (Potužák et al., 2007; Rutegwa et al., 2019) and
322 promotes oxygen consumption and anaerobic decomposition in the sediments (Baxa et al., 2020), leading to
323 enhanced CH₄ production (Bastviken et al., 2004; Grasset et al., 2018). In aquaculture ponds in Southeast China,
324 CH₄ fluxes exhibited considerable spatial variations and peaked in the relatively deep feeding zone, where the
325 large loads of sediment organic matter fueled CH₄ production (Yang et al., 2020). Furthermore, sediment
326 temperature was the strongest predictor of CH₄ fluxes in ponds (DelSontro et al., 2016; Yang et al., 2020). It is,
327 therefore, reasonable to assume that both temperature and oxygen concentration in the sediment likely contributed
328 to changes in observed CH₄ fluxes during the studied period in our study. Although both parameters were not
329 directly measured in the sediment, it can be deduced from their vertical profiles that the probability of sediment
330 anoxia was highest in August and lowest in September, and the sediment temperature was lowest in September
331 (see Fig. 5).

332 Our results agree with the generally accepted view that processes other than diffusive fluxes – most likely
333 ebullition – represent the major CH₄ pathway to the atmosphere in hyper-eutrophic ponds (Kosten et al., 2020).
334 Although freshwaters with high primary production are more likely to have high CH₄ ebullition rates (DelSontro
335 et al., 2016), the dominant role of ebullition was also found across lentic systems differing in size, trophic status
336 or geographical location (Aben et al., 2017). Ebullition accounted on average for 56 % of total CH₄ fluxes in
337 northern ponds in Canada (DelSontro et al., 2016), 49 and 71 % in two different zones of Lake Taihu (Xiao et al.,
338 2017) and 48-83 % in three Swedish lakes (Natchimuthu et al., 2016; Jansen et al., 2019). The highest contribution
339 was found in the small hyper-eutrophic Priest Pot (UK), where ebullition represented 96 % of the total CH₄ flux
340 from the pond (Casper et al., 2000). Apparently, the contribution of ebullition can vary among systems and will
341 remain uncertain until measurement designs cover enough spatiotemporal variability to yield representative values
342 for the whole ecosystem.

343 In shallow water bodies, a semi-stable flux of microbubbles was suggested to account for a significant portion of
344 the total CH₄ flux (Prairie and del Giorgio, 2013). When CH₄ concentration in the water column is above a certain



345 threshold of microbubble density, these microbubbles likely aggregate, fuse, and escape to the atmosphere from
346 buoyancy (Prairie and del Giorgio, 2013). Even a small fluctuation in hydrostatic pressure (e.g., due to changes in
347 atmospheric pressure) or lake water level was shown to trigger enhanced CH₄ ebullition (Bastviken et al., 2004;
348 Casper et al., 2000; Varadharajan and Hemond, 2012). Since ebullition rates increase exponentially with
349 temperature, CH₄ fluxes tend to peak in warm summer months (van Bergen et al., 2019). In our study, 1 % lower
350 air pressure in July and August than in September, along with bottom anoxia and higher water temperature, could
351 account for the enhanced release of CH₄ bubbles from the sediment (31.7 mmol m⁻²d⁻¹, >90 % of total CH₄ fluxes;
352 Suppl. Fig. 2). In September, when we observed the lowest water temperatures from the studied period and the
353 oxygen profile was rather uniform, ebullition accounted for 81 % (11 mmol m⁻²d⁻¹) of the total CH₄ fluxes. The
354 spatially pooled data of the total CH₄ fluxes measured in the Dehtář fishpond varied from 11.8 to 34.5 mmol m⁻²
355 d⁻¹, which is comparable with similar systems elsewhere (e.g., Bastviken et al., 2010; van Bergen et al., 2019;
356 Baron et al., 2022). To sum up, both diffusive fluxes and ebullition must be addressed to understand the magnitude
357 of total aquatic CH₄ fluxes and how their relative contributions vary across and within aquatic systems (Kosten et
358 al., 2020). Moreover, with an improved determination of CH₄ hot-spots and its causes, the management of ponds
359 could be changed accordingly and so the overall emissions reduced for example by decreasing P-availability and
360 dredging (Nijman et al., 2022).

361 **4.2 Effect of wind event on ecosystem spatial structure**

362 Sudden changes in ecosystem spatial structure in response to meteorological forcing have rarely been documented
363 (Loken et al., 2019) since they are hard to predict. Research into them using traditional methods requires intensive
364 effort or expensive instrumentation (Ortiz and Wilkinson, 2021), and it remains a matter of luck to obtain a relevant
365 dataset. In the July sampling campaign, we observed a strong impact of the wind on environmental heterogeneity
366 in the fishpond, which was apparent at a sub-daily time scale. Due to the methodological constraints, i.e., lack of
367 initial measurement, we can only speculate about the effect of wind on the total CH₄ fluxes. The northwest wind
368 during the day advected warmed surface water with cyanobacterial bloom from the north basin to the south. In the
369 evening, it resulted in bloom accumulation on the upward side and a north-south gradient of more than 4 °C and
370 4-24 mg L⁻¹ oxygen. After the winds fell off, the observed gradients declined during cooling at night. We assume
371 that the wind blowing across the pond surface drove buoyant cyanobacteria and surface water downwind and
372 caused an upwelling of deeper, colder, and hypoxic water on the upwind side. This wind-related circulation pattern
373 has been described as a “conveyor belt” in classical textbooks (Reynolds et al., 2006), held responsible for a
374 disruption of the thermal structure of the water column and the non-uniform spatial distribution of pH, oxygen,



375 CO₂ or CH₄ and also plankton assemblages (e.g. Loken et al., 2019; Natchimuthu et al., 2016; Rinke et al., 2009;
376 Ortiz and Wilkinson, 2021).

377 Similar to our study, mild winds (~4 m s⁻¹) were strong enough to redistribute heat and induce lake-wide
378 circulations driving upwelling and downwelling in 24 m deep Lake Pleasant (Czikowsky et al., 2018). As the wind
379 blows harder and lasts longer, the effects on ecosystem functioning may target higher trophic levels and become
380 more complex (Rinke et al., 2009). In Lake Constance, a three day storm event with wind velocities of ~10 m s⁻¹
381 resulted in a lake-wide displacement of water masses and the formation of the 6-15 °C horizontal surface water
382 gradient, which in turn changed the spatial distribution of phytoplankton, zooplankton and juvenile fish (Rinke et
383 al., 2009). After several stormy days (wind velocities of 12-15 m s⁻¹), Čech et al. (2011) observed negative effects
384 of wind-driven changes in water temperature and wave action on perch (*Perca fluviatilis*) spawning in the Lake
385 Milada. Although wind events affect shallow and deep lakes differently, there is growing evidence that they can
386 have far-reaching consequences on the functioning of aquatic ecosystems by disrupting energy flows, nutrient
387 fluxes, productivity and reproduction, and consequently altering community composition and trophic interactions
388 in the short and long term (Stockwell et al., 2020). As the frequency, intensity, spatial extent and duration of these
389 extreme meteorological events are projected to increase due to ongoing climate change (Comou and Rahmstorf,
390 2012), there is an urgent need to better understand the mechanisms underlying their impacts on the maintenance
391 of the ecosystem services.

392 **4.3 Summer changes in the oxygen regime**

393 Our data demonstrate that shallow, hyper-eutrophic ponds have disrupted oxygen regimes (Baxa et al., 2021) with
394 anoxic hypolimnion and may experience severe whole-water column hypoxia critical for aquatic biota (Miranda
395 et al., 2001). The hypoxic periods may result, for example, from sudden weather change (Jeppesen et al., 1990)
396 and last several days, during which physical processes and phytoplankton photosynthesis cannot compensate for
397 intense community respiration (Baxa et al., 2021). This became obvious in August when severe oxygen depletion
398 was measured at the surface across the whole pond, mostly far below a critical level of 4.5 mg L⁻¹, when adverse
399 effects came into play (Banerjee et al., 2019). However, oxygen surface concentrations in shallow parts of the
400 pond were substantially higher regardless of the time of day, which contrasts with findings of Miranda et al. (2001),
401 who emphasised shallow waters as the most sensitive parts of lakes, where hypoxic events can occur due to the
402 respiration of sediment biota. The observed spatial gradients of oxygen may create temporal refugia which allow
403 fish to survive harsh conditions that occur in the deepest part of the pond. To minimise economic losses and
404 negative impacts on the ecosystem, future research should identify the interplay between meteorological forcing,



405 trophic status and anthropogenic pressures (e.g. management practices) that affect oxygen fluctuations at various
406 time scales.

407 **4.4 Study limitations**

408 Like in other research, there are some limitations in the current study. Since our measurement had only a limited
409 temporal resolution (three samplings during the summer season), it is not appropriate to extrapolate CH₄ emissions
410 for annual values. Noticeably, future research must increase the frequency of the sampling and include also
411 innovative techniques to measure CH₄ fluxes at multiple fishponds, with different management regime. In our
412 study, the 12 h deployment time of the floating chambers could have led to extensive gas accumulation, which in
413 turn might have resulted in an underestimation of the total CH₄ fluxes due to the dissolution of the CH₄ from the
414 chamber into the water once the equilibrium concentration in the chamber is overcome (Bastviken et al., 2010).
415 However, CH₄ concentrations in water corresponded to a supersaturation of several orders of magnitude, so the
416 introduced bias appears to be of minor importance. In any case, our daily CH₄ fluxes represent a rather conservative
417 estimate for the global methane budget. In our study, we also did not address the important processes that could
418 shed light on the lake CH₄ budget, such as CH₄ oxidation rates (Bastviken et al., 2008) or biological interaction
419 (e.g. protistan grazing on CH₄ oxidising bacteria) in aquatic food webs (Sanseverino et al., 2012) that can affect
420 the overall CH₄ fluxes. We also lack information about spatial differences in sediment microbiota and organic
421 carbon content and compositions, which were found to affect CH₄ production rates (Berberich et al., 2020;
422 Emerson et al., 2021). Despite the limitation mentioned above, our results show that complementary spatial
423 surveys help contextualise the fixed station dynamics and provide additional, management-relevant information
424 about the fishpond.

425 **5. Conclusions**

426 Deciphering the mechanisms that drive spatial and temporal heterogeneity in aquatic ecosystem structure and
427 function not only expands our understanding of pond ecology but also provides insights to improve the
428 management of these ecosystems and the services they provide. Our results suggest that spatial heterogeneity needs
429 to be considered when designing experiments and monitoring programs. Without the spatially resolved sampling,
430 we introduce bias into our datasets, hampering our limnological understanding of the ecosystem's functioning and
431 impeding our ability to accurately estimate rates such as methane emissions on a global scale (DelSontro et al.,
432 2018a). In agreement with Kosten et al. (2020), we demonstrated that neglecting ebullition leads to a considerable
433 underestimating of the total CH₄ fluxes. Since there are thousands of these intensively managed fishponds, we



434 argue for changing the management practices toward sustainable use of natural resources to mitigate the overall
435 emissions of greenhouse gases from these ecosystems. Future studies are needed to characterise CH₄ fluxes over
436 a greater number and diversity of aquaculture ponds and examine the mechanisms controlling CH₄ emissions in
437 aquatic ecosystems.

438 **Acknowledgements**

439 The study was supported by the Czech Science Foundation (Research Projects No. 17-09310S, 19-23261S and
440 P504/19-16554S). We thank Dr. Martin Rulík for providing us gas chambers. We especially thank to Prof.
441 Miloslav Šimek and Linda Jiřová for enabling gas analyses. We are grateful Anna Sieczko for consultation on the
442 calculation of CH₄ fluxes. English correction was made by Anton Baer.

443 **Data availability**

444 Dataset associated with the manuscript can be found in the GitHub Repositories under
445 <https://zenodo.org/badge/latestdoi/587640213>.

446 **Author contributions**

447 All authors contributed to the study conception and design. PZ planned the campaign; PZ, AM and JN performed
448 the sampling and analyzed the data; AM performed the gas-measurements; VK performed statistical analyses and
449 modelling; PZ and AM wrote the manuscript. All authors read and approved the final manuscript.

450 **References**

- 451 Aben, R.C.H., Barros, N., van Donk, E., Frenken, T., Hilt, S., Kazanjian, G., Lamers, L.P.M., Peeters, E.T.H.M.,
452 Roelofs, J.G. M, de Senerpont Domis, L.N., Stephan, S., Velthuis, M., Van de Waal, D.B., Wik, M., Thornton,
453 B.F., Wilkinson, J., DelSontro, T., and Kosten, S.: Cross continental increase in methane ebullition under climate
454 change. *Nat. Commun.*, 8, 1682, <https://doi.org/10.1038/s41467-017-01535-y>, 2017.
- 455 Banerjee, A., Chakrabarty, M., Rakshit, N., Bhowmick, A.R., and Ray, S.: Environmental factors as indicators of
456 dissolved oxygen concentration and zooplankton abundance: deep learning versus traditional regression approach.
457 *Ecol. Indic.*, 100, 99-117, <https://doi.org/10.1016/j.ecolind.2018.09.051>, 2019.
- 458 Baron, A.A.P., Dyck, L.T., Amjad, H., Bragg, J., Kroft, E., Newson, J., Oleson, K., Casson, N.J., North, R.L.,
459 Venkiteswaran, J.J., and Whitfield, C.J.: Differences in ebullitive methane release from small, shallow ponds
460 present challenges for scaling. *Sci. Total Environ.*, 802, 149685, <https://doi.org/10.1016/j.scitotenv.2021.149685>,
461 2022.



- 462 Bartosiewicz, M., Maranger, R., Przytulska, A., and Laurion, I.: Effects of phytoplankton blooms on fluxes and
463 emissions of greenhouse gases in a eutrophic lake. *Water Res.*, 196, 116985,
464 <https://doi.org/10.1016/j.watres.2021.116985>, 2021.
- 465 Bastviken, D., Cole, J., Pace M., and Tranvik, L.: Methane emissions from lakes: Dependence of lake
466 characteristics, two regional assessments, and a global estimate. *Global Biogeochem. Cycles*, 18, GB4009,
467 <https://doi.org/10.1029/2004GB002238>, 2004.
- 468 Bastviken, D., Cole, J.J., Pace, M.L., and Van de Bogert, M.C.: Fates of methane from different lake habitats:
469 connecting whole-lake budgets and CH₄ emissions. *J. Geophys. Res. Biogeosci.*, 113, G02024,
470 <https://doi.org/10.1029/2007JG000608>, 2008.
- 471 Bastviken, D., Santoro, A.L., Marotta, H., Pinho, L.Q., Calheiros, D.F., Crill, P., and Enrich-Prast, A.: Methane
472 Emissions from Pantanal, South America, during the Low Water Season: Toward More Comprehensive Sampling.
473 *Environ. Sci. Tech.*, 44, 5450-5455, <https://doi.org/10.1021/es1005048>, 2010.
- 474 Bates, D., Maechler, M., Bolker, B., and Walker, S.: Fitting Linear Mixed-Effects Models Using lme4. *J. Stat.*
475 *Soft.*, 67, 1-48, <https://doi.org/10.18637/jss.v067.i01>, 2015.
- 476 Baxa, M., Musil, M., Kummel, M., Hazlík, O., Tesařová, B., and Pechar, L.: Dissolved oxygen deficits in a shallow
477 eutrophic aquatic ecosystem (fishpond) – Sediment oxygen demand and water column respiration alternately drive
478 the oxygen regime. *Sci. Total Environ.*, 766, 142647, <https://doi.org/10.1016/j.scitotenv.2020.142647>, 2021.
- 479 Beaulieu, J.J., DelSontro, T., and Downing, J.A.: Eutrophication will increase methane emissions from lakes and
480 impoundments during the 21st century. *Nat. Commun.*, 10, 3-7, <https://doi.org/10.1038/s41467-019-09100-5>,
481 2019.
- 482 Berberich, M.E., Beaulieu, J.J., Hamilton, T.L., Waldo, S., and Buffam, I.: Spatial variability of sediment methane
483 production and methanogen communities within a eutrophic reservoir: Importance of organic matter source and
484 quantity. *Limnol. Oceanogr.*, 65, 1336-1358, <https://doi.org/10.1002/lno.11392>, 2020.
- 485 Bižić, M., Klintzsch, T., Ionescu, D., Hindiyeh, M.Y., Günthel, M., Muro-Pastor, A.M., Eckert, W., Urich, T.,
486 Keppler, F., and Grossart, H.P.: Aquatic and terrestrial cyanobacteria produce methane. *Sci. Adv.*, 6, 1-10,
487 <https://doi.org/10.1126/sciadv.aax5343>, 2020.
- 488 Bussmann, I., Matoušů, A., Osudar, R., and Mau, S.: Assessment of the radio ³H-CH₄ tracer technique to measure
489 aerobic methane oxidation in the water column. *Limnol. Oceanogr.- Meth.*, 13, 312-327,
490 <https://doi.org/10.1002/lom3.10027>, 2015.
- 491 Casper, P., Maberly, S.C., Hall, G.H., and Finlay, B.J.: Fluxes of methane and carbon dioxide from a small
492 productive lake to the atmosphere. *Biogeochemistry*, 49, 1-19, <https://doi.org/10.1023/A:1006269900174>, 2000.
- 493 Čech, M., Peterka, J., Říha, M., Muška, M., Hejzlar, J., and Kubečka, J.: Location and timing of the deposition of
494 eggs strands by perch (*Perca fluviatilis* L.): the roles of lake hydrology, spawning substrate and female size.
495 *Knowl. Manag. Aquat. Ecosyst.*, 403, 1-12, <https://doi.org/10.1051/kmae/2011070>, 2011.
- 496 Céréghino, R., Biggs, J., Oertli, B., and Declerck, S.: The ecology of European ponds: defining the characteristics
497 of a neglected freshwater habitat. *Hydrobiologia*, 597, 1-6, <https://doi.org/10.1007/s10750-007-9225-8>, 2008.
- 498 Coumou, D. and Rahmstorf, S.: A decade of weather extreme. *Nat. Clim. Change*, 2, 491-96,
499 <https://doi.org/10.1038/nclimate1452>, 2012.
- 500 Crusius, J. and Wanninkhof, R.: Gas transfer velocities measured at low wind speed over a lake. *Limnol. Oceanogr.*,
501 48, 1010-1017, <https://doi.org/10.4319/lo.2003.48.3.1010>, 2003.



- 502 Czikowsky, M.J., MacIntyre, S., Tedford, E.W., Vidal, J., and Miller, S.D.: Effects of wind and buoyancy on
503 carbon dioxide distribution and air-water flux of a stratified temperate lake. *J. Geophys. Res. Biogeosci.*, 123,
504 2305-2322, <https://doi.org/10.1029/2017JG004209>, 2018.
- 505 De Meester, L., Declerck, S., Stoks, R., Louette, G., Van de Meutter, F., De Bie, T., Michels, E., and Brendonck,
506 L.: Ponds and pools as model systems in conservation biology, ecology and evolutionary biology. *Aquat. Cons.*,
507 15, 715-725, <https://doi.org/10.1002/aqc.748>, 2005.
- 508 DelSontro, T., Boutet, L., St-Pierre, A., del Giorgio, P.A., and Prairie, Y.T.: Methane ebullition and diffusion from
509 northern ponds and lakes regulated by the interaction between temperature and system productivity. *Limnol.*
510 *Oceanogr.*, 61, 62-77, <https://doi.org/10.1002/lno.10335>, 2016.
- 511 DelSontro, T., Beaulieu, J.J., and Downing, J.J.: Greenhouse gas emissions from lakes and impoundments:
512 upscaling in the face of global change. *Limnol. Oceanogr. Lett.*, 3, 64-75, <https://doi.org/10.1002/lo12.10073>,
513 2018a.
- 514 DelSontro, T., del Giorgio, P.A., and Prairie, Y.T.: No Longer a Paradox: The Interaction Between Physical
515 Transport and Biological Processes Explains the Spatial Distribution of Surface Water Methane Within and Across
516 Lakes. *Ecosystems*, 21, 1073-1087, [10.1007/s10021-017-0205-1](https://doi.org/10.1007/s10021-017-0205-1), 2018b.
- 517 Emerson, J.B., Varner, R.K., Wik, M., Parks, D.H., Neumann, R.B., Johnson, J.E., Singleton, C. M., Woodcroft,
518 B.J., Tollerson II, R., Owusu-Domney, A., Binder, M., Freitas, N. L., Crill, P.M., Saleska, S.R., Tyson, G.W., and
519 Rich, V.I.: Diverse sediment microbiota shape methane emission temperature sensitivity in Arctic lakes. *Nat.*
520 *Commun.*, 12, 5815, <https://doi.org/10.1038/s41467-021-25983-9>, 2021.
- 521 Grasset, Ch., Mendonça, R., Saucedo, G.V., Bastviken, D., Roland, F., and Sobek, S.: Large but variable methane
522 production in anoxic freshwater sediment upon addition of allochthonous and autochthonous organic matter.
523 *Limnol. Oceanogr.*, 63, 1488-1501, <https://doi.org/10.1002/lno.10786>, 2018.
- 524 Halekoh, H. and Hojsgaard, S.: A Kenward-Roger Approximation and Parametric Bootstrap Methods for Tests in
525 Linear Mixed Models - The R Package pbrtest. *J. Stat. Soft.*, 59, 1-30, <https://doi.org/10.18637/jss.v059.i09> 2014.
- 526 Hofmann, H., Federwisch, L., and Peeters, F.: Wave-induced release of methane: littoral zones as a source of
527 methane in lakes. *Limnol. Oceanogr.*, 55, 1990-2000, <https://doi.org/10.4319/lo.2010.55.5.1990>, 2010.
- 528 Hofmann, H.: Spatiotemporal distribution patterns of dissolved methane in lakes: How accurate are the current
529 estimations of the diffusive flux path? *Geophys. Res. Lett.*, 40, 2779-2784, <https://doi.org/10.1002/grl.50453>,
530 2013.
- 531 Hu, Z., Wu, S., Ji, Ch., Zou, J., Zhou, Q., and Liu, S.: A comparison of methane emissions following rice paddies
532 conversion to crab-fish farming wetlands in southeast China. *Environ. Sci. Pollut. Res.*, 23, 1505-1515,
533 <https://doi.org/10.1007/s11356-015-5383-9>, 2016.
- 534 Jansen, J., Thornton, B.F., Jammet, M.M., Wik, M., Cortés, A., Friborg, T., MacIntyre, S., and Crill, P.M.:
535 Climate-sensitive controls on large spring emissions of CH₄ and CO₂ from northern lakes. *J. Geophys. Res.*,
536 *Biogeosciences*, 124, 2379-2399, <https://doi.org/10.1029/2019JG005094>, 2019.
- 537 Jeppesen, E., Søndergaard, M., Sortkjaer, O., Mortensen, E., and Kristensen, P.: Interactions between
538 phytoplankton zooplankton and fish in a shallow hypertrophic Lake a study of phytoplankton collapses in Lake
539 Sobygaard, Denmark. *Hydrobiologia*, 1991, 149-164, <https://doi.org/10.1007/BF00026049>, 1990.
- 540 Kolar, V., Vlašánek, P., and Boukal, D.S.: The influence of successional stage on local odonate communities in
541 man-made standing waters. *Ecol. Eng.*, 173, 106440, <https://doi.org/10.1016/j.ecoleng.2021.106440>, 2021.



- 542 Kopáček, J. and Hejzlar, J.: Semi-micro determination of total phosphorus in fresh waters with perchloric acid
543 digestion. *Int. J. Environ. Anal. Chem.*, 53, 173-183, <https://doi.org/10.1080/03067319308045987>, 1993.
- 544 Kopáček, J. and Procházková, L.: Semi-Micro Determination of Ammonia in Water by the Rubazotic Acid Method.
545 *Int. J. Environ. Anal. Chem.*, 53, 243-248, <https://doi.org/10.1080/03067319308045993>, 1993.
- 546 Kosten, S., Almeida, R.M., Barbosa, I., Mendonça, R., Muzitano, I.S., Oliveira-Junior, E.S., Vroom, R.J.E., Wang,
547 H.J., and Barros, N.: Better assessments of greenhouse gas emissions from global fish ponds needed to adequately
548 evaluate aquaculture footprint. *Sci. Total Environ.*, 748, 141247, <https://doi.org/10.1016/j.scitotenv.2020.141247>,
549 2020.
- 550 Laas, A., Noges, P., Koiv, T., and Noges, T.: High-frequency metabolism study in a large and shallow temperate
551 lake reveals seasonal switching between net autotrophy and net heterotrophy. *Hydrobiologia*, 694, 57-74,
552 <https://doi.org/10.1007/s10750-012-1131-z>, 2012.
- 553 Loken, L.C., Crawford, J.T., Schramm, P.J., Stadler, P., Desai, A.R., and Stanley, E.H.: Large spatial and temporal
554 variability of carbon dioxide and methane in a eutrophic lake. *J. Geophys. Res. Biogeosci.*, 124, 2248-2266
555 <https://doi.org/10.1029/2019JG005186>, 2019.
- 556 Lüdecke, D.: “ggeffects: Tidy Data Frames of Marginal Effects from Regression Models.” *J. Open Source Soft.*,
557 3, 772, <https://doi.org/10.21105/joss.00772>, 2018.
- 558 Lüdecke, D., Makowski, D., and Waggoner, P.: performance: Assessment of Regression Models Performance. R
559 package version 0.4.4. <https://CRAN.R-project.org/package=performance>, 2020.
- 560 Ma, Y., Sun, L., Liu, C., Yang, X., Zhou, W., Yang, B., Schwenke, G., and Liu, D.L.: A comparison of methane
561 and nitrous oxide emissions from inland mixed-fish and crab aquaculture ponds. *Sci. Total Environ.*, 637-638,
562 517-523, <https://doi.org/10.1016/j.scitotenv.2018.05.040>, 2018
- 563 McAuliffe, C.: Gas Chromatographic determination of solutes by multiple phase equilibrium. *Chem. Technol.*, 1,
564 46-51, 1971.
- 565 Miranda, L.E., Hargreaves, J.A., and Raborn, S.W.: Predicting and managing risk of unsuitable dissolved oxygen
566 in a eutrophic lake. *Hydrobiologia*, 457, 177-185, <https://doi.org/10.1023/A:1012283603339>, 2001.
- 567 Murphy, J. and Riley, J.P.: A modified single-solution method for the determination of phosphate in natural waters.
568 *Anal. Chim. Acta*, 27, 31-36, [https://doi.org/10.1016/S0003-2670\(00\)88444-5](https://doi.org/10.1016/S0003-2670(00)88444-5), 1962.
- 569 Natchimuthu, S., Sundgren, I., Gålfalk, M., Klemedtsson, L., Crill, P., Danielsson, Å., and Bastviken, D.: Spatio-
570 temporal variability of lake CH₄ fluxes and its influence on annual whole lake emission estimates. *Limnol.*
571 *Oceanogr.*, 61, 13-26, <https://doi.org/10.1002/lno.10222>, 2016.
- 572 Nijman, T.P.A., Lemmens, M., Lurling, M., Kosten, S., Welte, C., and Veraart, A.J.: Phosphorus control and
573 dredging decrease methane emissions from shallow lakes. *Sci. Total Environ.*, 847, 15758,
574 <https://doi.org/10.1016/j.scitotenv.2022.157584>, 2022.
- 575 Ortiz, D.A. and Wilkinson, G.M.: Capturing the spatial variability of algal bloom development in a shallow
576 temperate lake. *Freshwater Biol.*, 66, 2064-2075, <https://doi.org/10.1111/fw.13814>, 2021.
- 577 Ostrovsky, I., McGinnis, D.F., Lapidus, L., and Eckert, W.: Quantifying gas ebullition with echosounder: The role
578 of methane transport by bubbles in a medium-sized lake. *Limnol. Oceanogr. Meth.*, 6, 105-118,
579 <https://doi.org/10.4319/lom.2008.6.105>, 2008.
- 580 Pechar, L.: Impacts of long-term changes in fishery management on the trophic level and water quality in Czech
581 fishponds. *Fisheries Manag. Ecol.*, 7, 23-32, [10.1046/j.1365-2400.2000.00193.x](https://doi.org/10.1046/j.1365-2400.2000.00193.x), 2000.



- 582 Pokorný, J. and Hauser, V.: The restoration of fish ponds in agricultural landscapes. *Ecol. Eng.*, 18, 555-574,
583 [https://doi.org/10.1016/S0925-8574\(02\)00020-4](https://doi.org/10.1016/S0925-8574(02)00020-4), 2002.
- 584 Potužák, J., Hůda, J., and Pechar, L.: Changes in fish production effectivity in eutrophic fishponds – impact of
585 zooplankton structure. *Aquacult. Int.*, 15, 201-210, <https://doi.org/10.1007/s10499-007-9085-2>, 2007.
- 586 Potužák, J., Duras, J., and Drozd, B.: Mass balance of fishponds: are they sources or sinks of phosphorus?
587 *Aquacult. Int.*, 24, 1725-1745, <https://doi.org/10.1007/s10499-016-0071-4>, 2016.
- 588 Prairie, Y.T. and del Giorgio, P.A.: A new pathway of freshwater methane emissions and the putative importance
589 of microbubbles. *Inland Waters*, 3, 311-320, <https://doi.org/10.5268/IW-3.3.542>, 2013.
- 590 Procházková, L.: Bestimmung der Nitrate im Wasser. *Zeitschrift für Analytische Chemie*, 167, 254-260, 1959.
- 591 Rasilo, T., Prairie, Y.T., and del Giorgio, P.A.: Large-scale patterns in summer diffusive CH₄ fluxes across boreal
592 lakes, and contribution to diffusive C emissions. *Glob. Change Biol.*, 21, 1124-1139,
593 <https://doi.org/10.1111/gcb.12741>, 2015.
- 594 R Core Team: A language and environment for statistical computing. R Foundation for Statistical Computing.
595 Vienna, Austria <https://www.R-project.org/>, 2018.
- 596 Reynolds, C.S.: *Ecology of phytoplankton*, Cambridge University Press, Cambridge,
597 <https://doi.org/10.1017/CBO9780511542145>, 2006.
- 598 Rinke, K., Huber, A.M.R., Kempke, S., Eder, M., Wolf, T., Probst, W.N., and Rothhaupt, K.: Lake-wide
599 distributions of temperature, phytoplankton, zooplankton, and fish in the pelagic zone of a large lake. *Limnol.*
600 *Oceanogr.*, 54, 1306-1322, <https://doi.org/10.4319/lo.2009.54.4.1306>, 2009.
- 601 Rutegwa, M., Potužák, J., Hejzlar, J., and Drozd, B.: Carbon metabolism and nutrient balance in a hypereutrophic
602 semi-intensive fishpond. *Knowl.Manag. Aquat. Ecosyst.*, 49, <https://doi.org/10.1051/kmae/2019043>, 2019.
- 603 Sanseverino, A.M., Bastviken, D., Sundh, I., Pickova, J., and Enrich-Prast, A.: Methane carbon supports aquatic
604 food webs to the fish level. *PLoS One*7, e42723, <https://doi.org/10.1371/journal.pone.0042723>, 2012.
- 605 Scheffer, M.: *Ecology of shallow lakes. Population and Community Biology Series*. Springer, 357 p.,
606 <https://doi.org/10.1007/978-1-4020-3154-0>, 2004.
- 607 Schilder, J., Bastviken, D., van Hardenbroek, M., Kankaala, P., Rinta, P., Stötter, T., and Heiri, O.: Spatial
608 heterogeneity and lake morphology affect diffusive greenhouse gas emission estimates of lakes. *Geophys. Res.*
609 *Lett.*, 40, 5752-5756, <https://doi.org/10.1002/2013GL057669>, 2013.
- 610 Schmiedeskamp, M., Praetzel, L.S.E., Bastviken, D., and Knorr, K.H.: Whole-lake methane emissions from two
611 temperate shallow lakes with fluctuating water levels: Relevance of spatiotemporal patterns. *Limnol. Oceanogr.*,
612 66, 2455-2469, <https://doi.org/10.1002/lno.11764>, 2021.
- 613 Stanley, E.H., Collins, S.M., Lottig, N.R., Oliver, S.K., Webster, K.E., Cheruvilil, K.S., and Soranno, P.A.: Biases
614 in lake water quality sampling and implications for macroscale research. *Limnol. Oceanogr.*, 64, 1572-1585,
615 <https://doi.org/10.1002/lno.11136>, 2019.
- 616 Stockwell, J.D., Doubek, J.P., Adrian, R., Anneville, O., Carey, C.C., Carvalho, L., Domis, L.N.D.S., Dur, G.,
617 Frassl, M.A., Grossart, H.-P., Ibelings, B.W., Lajeunesse, M.J., Lewandowska, A.M., Llamas, M.E., Matsuzaki,
618 S.-I.S., Nodine, E.R., Nöges, P., Patil, V.P., Pomati, F., Rinke, K., Rudstam, L.G., Rusak, J.A., Salmaso, N.,
619 Seltmann, C.T., Straile, D., Thackeray, S.J., Thiery, W., Urrutia-Cordero, P., Venail, P., Verburg, P., Woolway,
620 R.I., Zohary, T., Andersen, M.R., Bhattacharya, R., Hejzlar, J., Janatian, N., Kpodonu, A.T.N.K., Williamson,



- 621 T.J., and Wilson, H.L.: Storm impacts on phytoplankton community dynamics in lakes. *Glob. Change Biol.*, 26,
622 2756-2784, <https://doi.org/10.1111/gcb.15033>, 2020.
- 623 Tranvik, L.J., Downing, J.A., Cotner, J.B., Loiselle, S.A., Striegl, R.G., Ballatore, T.J., Dillon, P., Finlay, K.,
624 Fortino, K., Knoll, L.B., Kortelainen, P.L., Kutser, T., Larsen, S., Laurion, I., Leech, D.M., McCallister, S.L.,
625 McKnight, D.M., Melack, J.M., Overholt, E., Porter, J.A., Prairie, Y.T., Renwick, W.H., Roland, F., Sherman,
626 B.S., Schindler, D.W., Sobek, S., Tremblay, A., Vanni, M.J., Verschoor, A.M., von Wachenfeldt, E.,
627 Weyhenmeyer, G.A.: Lakes and reservoirs as regulators of carbon cycling and climate. *Limnol. Oceanogr.*, 54,
628 2298-2314, https://doi.org/10.4319/lo.2009.54.6_part_2.2298, 2009.
- 629 van Bergen, T.J.H.M., Barros, N., Mendonça, R., Aben, R.C.H., Althuizen, I.H.J., Huszar, V., Lamers, L.P.M.,
630 Lüring, M., Roland, F., Kosten, S.: Seasonal and diel variation in greenhouse gas emissions from an urban pond
631 and its major drivers. *Limnol. Oceanogr.*, 64, 2129-2139, <https://doi.org/10.1002/lno.11173>, 2019.
- 632 Varadharajan, Ch. and Hemond, H.F.: Time-series analysis of high-resolution ebullition fluxes from a stratified,
633 freshwater lake. *J. Geophys. Res.*, 117, G02004, <https://doi.org/10.1029/2011JG001866>, 2012.
- 634 Wanninkhof, R.: Relationship between wind speed and gas exchange over the ocean revisited. *Limnol. Oceanogr.*
635 *Methods*, 12, 351-362, <https://doi.org/10.4319/lom.2014.12.351>, 2014.
- 636 Wiesenburg, D.A. and Guinasso N.L.: Equilibrium solubilities of methane, carbon monoxide, and hydrogen in
637 water and sea water. *J. Chem. Eng. Data*, 24, 356-360, <https://doi.org/10.1021/je60083a006>, 1979.
- 638 Wik, M., Varner, R.K., Anthony, K.W., MacIntyre, S., and Bastviken, D.: Climate-sensitive northern lakes and
639 ponds are critical components of methane release. *Nat. Geosci.*, 9, 99-105, <https://doi.org/10.1038/ngeo2578>,
640 2016.
- 641 Xiao, Q., Zhang, M., Hu, Z., Gao, Y., Hu, Ch., Liu, Ch., Liu, S., Zhang, Z., Zhao, J., Xiao, W., and Lee, X.: Spatial
642 variations of methane emission in a large shallow eutrophic lake in subtropical climate. *J. Geophys. Res.*
643 *Biogeosci.*, 122, <https://doi.org/10.1002/2017JG003805>, 2017.
- 644 Yamamoto, S., Alcauskas, J.B., and Crozier, T.E. Solubility of methane in distilled water and seawater. *J. Chem.*
645 *Eng. Data*, 21, 78-80, <https://doi.org/10.1021/je60068a029>, 1976.
- 646 Yan, X., Xu, X., Ji, M., Zhang, Z., Wang, M., Wu, S., Wang, G., Zhang, Ch., and Liu, H.: Cyanobacteria blooms:
647 A neglected facilitator of CH₄ production in eutrophic lakes. *Sci. Total Environ.*, 651, 466-474,
648 <https://doi.org/10.1016/j.scitotenv.2018.09.197>, 2019.
- 649 Yang, P., Zhang, Y., Yang, H., Zhang, Y., Xu, J., Tan, L., Tong, C., and Lai, D.Y.: Large fine-scale spatiotemporal
650 variations of CH₄ diffusive fluxes from shrimp aquaculture ponds affected by organic matter supply and aeration
651 in Southeast China. *J. Geophys. Res. Biogeosci.*, 124, 1290-1307, <https://doi.org/10.1029/2019JG005025>, 2019.
- 652 Yang, P., Zhang, Y., Yang, H., Guo, Q., Lai, D.Y.F., Zhao, G., Li, L., and Tong, C.: Ebullition was a major
653 pathway of methane emissions from the aquaculture ponds in Southeast China. *Water Res.*, 184, 116176,
654 <https://doi.org/10.1016/j.watres.2020.116176>, 2020.
- 655 Yuan, J., Xiang, J., Liu, D.Y., Kang, H., He, T.H., Kim, S., Lin, Y.X., Freeman, C., and Ding, W.X.: Rapid growth
656 in greenhouse gas emissions from the adoption of industrial-scale aquaculture. *Nat. Clim. Chang.*, 9, 318-322,
657 <https://doi.org/10.1038/s41558-019-0425-9>, 2019.
- 658 Yuan, J., Liu, D., Xiang, J., He, T., Kang, H., and Ding, W.: Methane and nitrous oxide have separated production
659 zones and distinct emission pathways in freshwater aquaculture ponds. *Water Research*, 190, 116739,
660 <https://doi.org/10.1016/j.watres.2020.116739>, 2021.



- 661 Zar, J.H.: Biostatistical analysis. Prentice Hall, Inc., Englewood Cliffs, New York, 663 p., 1984.
- 662 Zhang, L., Liao, Q., Gao, R., Luo, R., Liu, Ch., Zhong, J., and Wang, Z.: Spatial variations in diffusive methane
663 fluxes and the role of eutrophication in a subtropical shallow lake. *Sci. Total Environ.*, 759, 143495,
664 <https://doi.org/10.1016/j.scitotenv.2020.143495>, 2021.
- 665 Zhao, J., Zhang, M., Xiao, W., Jia, L., Zhang, X., Wang, J., Zhang, Z., Xie, Y., Yini Pu, Liu, S., Feng, Z., Lee X.:
666 Large methane emission from freshwater aquaculture ponds revealed by long-term eddy covariance observation.
667 *Agric. For. Meteorol.*, 308-309, 108600, <https://doi.org/10.1016/j.agrformet.2021.108600>, 2021.
- 668 Zhou, Y.Q., Zhou, L., Zhang, Y.L., de Souza, J.G., Podgorski, D.C., Spencer, R.G.M., Jeppesen, E., and Davidson,
669 T.A.: Autochthonous dissolved organic matter potentially fuels methane ebullition from experimental lakes. *Water*
670 *Res.*, 166, 115048, <https://doi.org/10.1016/j.watres.2019.115048>, 2019.
- 671 Zuur, A.F., Ieno, E.N., Walker, N.J., Saveliev, A.A., and Smith, G.M.: Mixed effects models and extensions in
672 ecology with R. Springer, New York, USA, 574 p, <https://doi.org/10.1007/978-0-387-87458-6>, 2009.
- 673